Ion-ion neutralization of iodine in radio-frequency inductive discharges of Xe and I_2 mixtures

Paul N. Barnes
Wright Laboratory, 2645 Fifth Street Ste 13, Wright-Patterson AFB, Ohio 45433-7919

Mark J. Kushner[a)]
Department of Electrical and Computer Engineering, University of Illinois, 1406 W. Green St., Urbana, Illinois 61801

(Received 16 April 1997; accepted for publication 22 May 1997)

Xe/I_2 low-pressure electric discharges are being developed as efficient, long-lived ultraviolet lighting sources. In this work the kinetics of low pressure, 0.5–5 Torr, radio-frequency inductively excited discharges sustained in Xe and I_2 were investigated to determine the source of radiating states. The diagnostics applied in this study include optical absorption and emission spectroscopy, microwave interferometry, and microwave absorption. We found that in time modulated discharges, the emissions from excited states of atomic iodine decays with time constants of hundreds of microseconds. These observations are consistent with those states being populated by ion-ion neutralization. Electron-ion recombination leading to excited states appears not to be an important source of emission. [S0021-8979(97)01117-1]

I. INTRODUCTION

Electrically efficient, compact ultraviolet (UV) lighting sources are being developed as possible replacements for mercury vapor lamps. Although highly efficient, the use of mercury in commercial lamps poses disposal and environmental problems. An efficient source of UV light that is more environmentally benign would be ideal. In this regard, lighting sources using a xenon/iodine gas mixture are being investigated as a multiwavelength UV lighting source. There is a considerable body of research investigating rare gas-halogen kinetics in the context of atmospheric pressure excimer lasers.[1] There has, however, been little work which addresses low pressure (0.5–5 Torr) systems in the context of average power lighting sources, and on formation of the XeI* exciplex[2–8] or the $I^*(^2P_{3/2})$ state[9–12] in particular.

In this work we have investigated low-pressure, inductively excited radio-frequency (rf) discharges in Xe/I_2 mixtures to determine the kinetics and radiative processes leading to UV emission from atomic and molecular iodine. In a previous work, we found that in this class of discharge (low-pressure, large I_2 mole fraction, quasicontinuous excitation), XeI(B) is likely formed through an inverse harpoon reaction between highly excited states of I_2 and Xe.[2] In higher pressure discharges, formation of XeI(B) is typically dominated by the direct harpoon reaction ($Xe^*+I_2 \rightarrow Xe(B)+I$). In this work, we measured densities of excited states during the afterglow of square wave modulated rf discharges with the goal of determining their sources. We found that excited states of I producing emission at 206 nm ($^2P_{3/2} \rightarrow {}^2P_{1/2}$) are likely populated by ion-ion neutralization between I^+ and I^-. The experimental apparatus is described in Sec. II, followed by a discussion of results in Sec. III. The concluding remarks are in Sec. IV.

a)Electronic mail: mjk@uiuc.edu

II. DESCRIPTION OF THE EXPERIMENTAL APPARATUS

The experimental apparatus has been previously discussed[2] and will be only briefly described here. The diagnostics we used to examine the discharge kinetics are emission spectroscopy, laser-induced fluorescence (LIF), optical absorption spectroscopy, microwave interferometry, and microwave absorption. The emission spectroscopy, LIF, and optical absorption diagnostics are described in Ref. 2. The electric discharge we investigated is an inductively excited system. The plasma is sustained in an 3.8 cm i.d. by 7.6-cm-long quartz tube. The excitation coil is a solenoid consisting of 0.64 cm diameter copper tubing with an axial length of 6.5 cm and inside diameter of 4.4 cm, and having eight and three-quarters turns. Variable rf power is supplied to the system at 11.3 MHz. Iodine crystals, 99.8% assay, are purified by several freeze, pump, thaw, and resublimation cycles in an iodine trap and isolated in a sidearm of the cell. Purification of the iodine is conducted prior to filling the discharge cells. After a cell is filled to the desired partial pressures of xenon and iodine, the quartz arm of the cell is sealed off. The cell was operated in a square wave pulse modulated mode having a 50% duty cycle and a repetition rate of 0.09 Hz–1 kHz. Although the discharge is powered by a coil, the electrical coupling may be either capacitive or inductive, and we will note the particular coupling in each case.

Microwave interferometry is used to measure electron density during the afterglow of modulated discharges as shown in Fig. 1. The klystron used to generate the microwaves is an OKI Electronics model 1591 powdered by an FXR, Inc. universal klystron power supply. The waveguide for delivery of the microwaves is rectangular with the dimension of 3.5 mm by 7 mm. The time variation of the electron density was measured by keeping the microwave frequency fixed (35 Ghz) and recording the amplitude of the combined reference leg-probe leg signal at the detector.

Microwave absorption for electron heating was also used as a diagnostic to detect the presence of electron-ion recom-

 0021-8979/97/82(5)/2150/6/$10.00

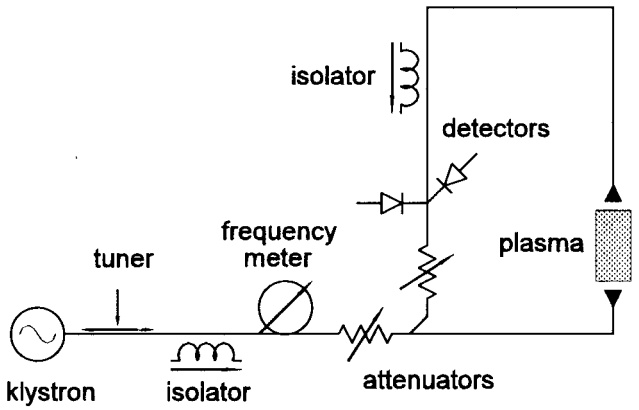

FIG. 1. Schematic of experimental apparatus for microwave interferometry.

bination during the afterglow as shown in Fig. 2. The klystron used to generate the microwaves for the microwave absorption diagnostic is a Varian X-13, emitting at 9 GHz. The microwaves were pulsed for a duration of 100 μs after rf power to the plasma is modulated off. Since the electron-ion recombination coefficient is inversely proportional to electron temperature, electron heating by the microwave pulse reduces electron loss by this process. An alternative heating method during the afterglow is not to fully modulate the rf power. The power is reduced below the minimum threshold for maintaining the discharge during the ''off'' phase, and is therefore not sufficient to cause ionizations, but does serve to heat the electrons and prevent them from becoming thermalized.

III. IODINE EMISSION FROM RF MODULATED DISCHARGES

In this section, we discuss kinetic process in rf modulated discharges in $Xe/I_2=5.0/0.3$ at a total pressure of 5.3 Torr. An energy level diagram of the pertinent states of Xe, I_2, and I is shown in Fig. 3. The time-dependent emission of $I_2^{**}(D'\rightarrow A')$ at 342 nm following termination of a 35 W discharge is displayed in Fig. 4(a). For these conditions, the discharge is operating in a capacitive mode. Emission at first

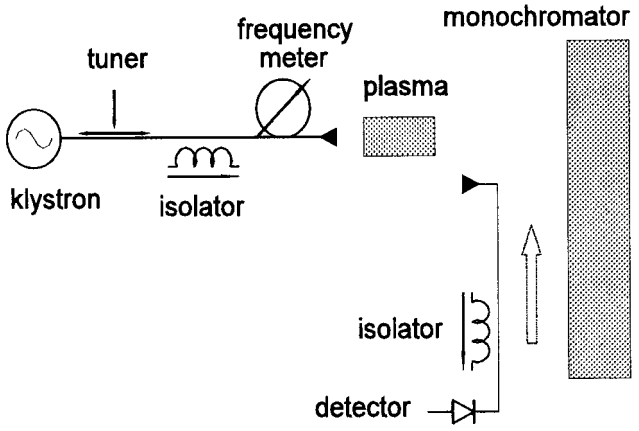

FIG. 2. Schematic of experimental apparatus for microwave absorption.

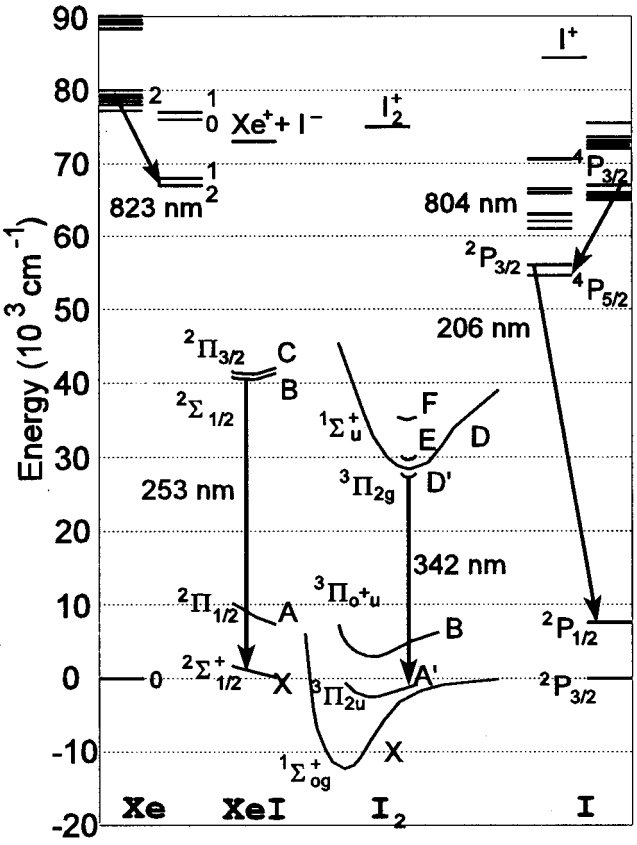

FIG. 3. Energy diagram of Xe, XeI, I_2, and I.

rapidly decays, in about 1.5 μs. The lifetimes of the excited states are 5–30 ns, therefore, emission over longer periods requires continued excitation. The electric time constant of the discharge circuit is $\approx$2 μs. Given the large electron collision frequency for these conditions ($\approx 3\times 10^9$ s^{-1}), the electron temperature can be expected to track the power deposition. The $\approx$2 μs decay time of the optical emission can therefore be attributed to the decay in power deposition and electron temperature.

The emission has a second long decay constant of hundreds of μs, which is barely discernible in the figure. The magnitude of the emission at the start of the longer decay period is typically a fraction of the emission at the beginning of the afterglow, in this case $\approx$4%. When operating at 70 W, the long-term decay is more discernible as shown in Fig. 4(b). (70 W is the maximum power deposition which can be maintained prior to the discharge switching to the inductively coupled mode.) The long time scale emission from these short-lived states must result from an energy transfer or recombination process since direct electron impact is not likely. Three such possibilities are excitation transfer from Xe($6s$) metastable states, ion-ion neutralization such as $I_2^+ + I^- \rightarrow I_2^{**} + I$, or electron-ion recombination such as $I_2^+ + e \rightarrow I^* + I$ followed by excitation transfer to I_2. Three-body processes are unlikely at the pressures used in this experiment.

The emission from the $I^*(^4P^0_{3/2})$ state at 804 nm following modulation of a 50 W plasma operating in the inductively coupled mode is displayed in Fig. 5. With the dis-

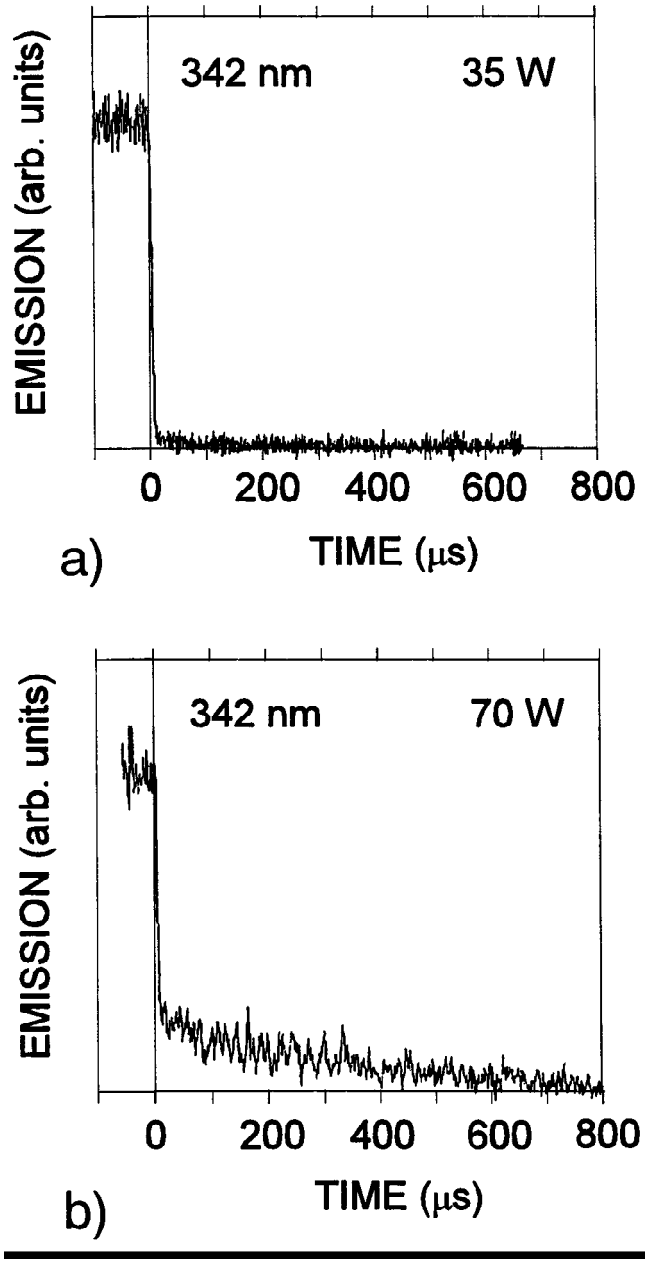

FIG. 4. $I_2^{**}(^3\Pi_{2g}\rightarrow{}^3\Pi_{2u})$ emission (342 nm) from a 0.5 Torr Xe/≈0.3 Torr I_2 time modulated discharge: (a) 35 W, (b) 70 W. Scaling is linear.

charge operating in the high-power inductive mode, the initial drop in emission is a smaller fraction of the total emission, and has a longer time scale of ≈15 μs than when operating in the capacitive mode. This short-term decay can also likely be attributed to thermalization of electrons. Although the relative magnitudes differ, we find that both in the capacitive and inductively coupled cases, there are two time scales for the decay of emission from excited states of iodine. The shorter time scale (a few - tens of μs) is associated with decay of power deposition and electron temperature. The longer time scale (tens of μs–hundreds of μs) must be associated with energy transfer processes (e.g., $Xe^*+I_2\rightarrow I_2^{**}+Xe$) or recombination/reassociation processes (e.g., $I^-+I^+\rightarrow I^*+I$ or $e + I_2^+\rightarrow I^*+I$).

The relative emission from excited states of Xe, I_2, and I during the afterglow of the modulated discharge are shown in Fig. 6. The discharge is operated in the inductive mode with 40 W of power deposition. A comparison between the emission from selected, but representative states of each species appears in Fig. 7. The time dependence of the density of the metastable state Xe(6s), as determined by optical absorption spectroscopy of the discharge, correlates well with the Xe excited state emission at 823 nm. The $^2P_{3/2}\rightarrow{}^2P_{1/2}$ emission of atomic iodine at 206 nm decays over hundreds of μs. After an initial rapid decay, associated with the decay of electron temperature and power deposition, the emission rebounds and has a second maximum. At higher powers, the 206 nm emission in the afterglow can exceed that during the powered portion of the cycle, as shown in Fig. 8. The behavior of the 206 nm emission decay can be attributed to how the $I(^2P_{3/2})$ state is populated as explained below.

The $I(^2P_{3/2})$state leading to emission at 206 nm during the afterglow could be formed by one of the following processes:

$$e+I_2^+\rightarrow I^{**}+e \qquad (1a)$$

$$\hookrightarrow I(^2P_{3/2}),$$

$$Xe(6s)+I_2\rightarrow I(^2P_{3/2})+Xe, \qquad (1b)$$

$$I^++I^-\rightarrow I(^2P_{3/2})+I. \qquad (1c)$$

The dissociative recombination of I_2^+ should be expected to populate a variety of atomic iodine excited states. If the $I(^2P_{3/2})$ state is formed largely by the electron-ion recombination (either dissociative or direct recombination of I^+) then one might expect that the time dependence of emission from higher states in atomic iodine would be similar to the $I(^2P_{3/2})$ emission at 206 nm. As shown in Fig. 6(b), this is not the case, which casts doubt on recombination as a source of the emission. To further test for this mechanism, we ap-

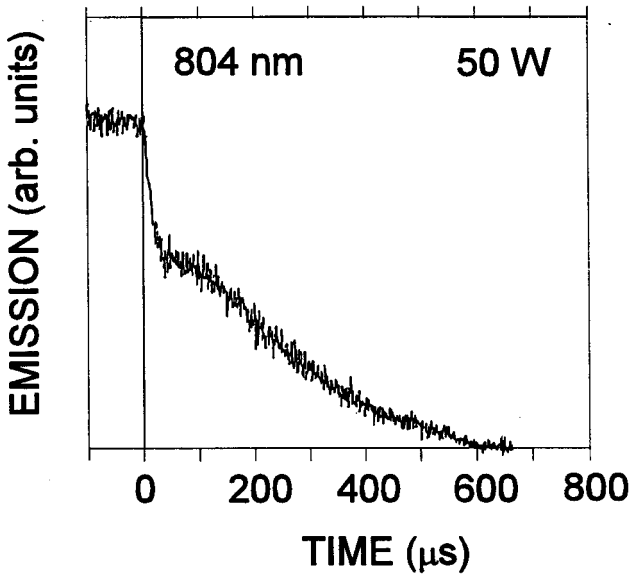

FIG. 5. $I^{**}(^4P^0_{3/2}\rightarrow{}^4P_{5/2})$emission (804 nm) at 50 W for a 0.5 Torr Xe/≈0.3 Torr I_2 time modulated discharge. Scaling is linear.

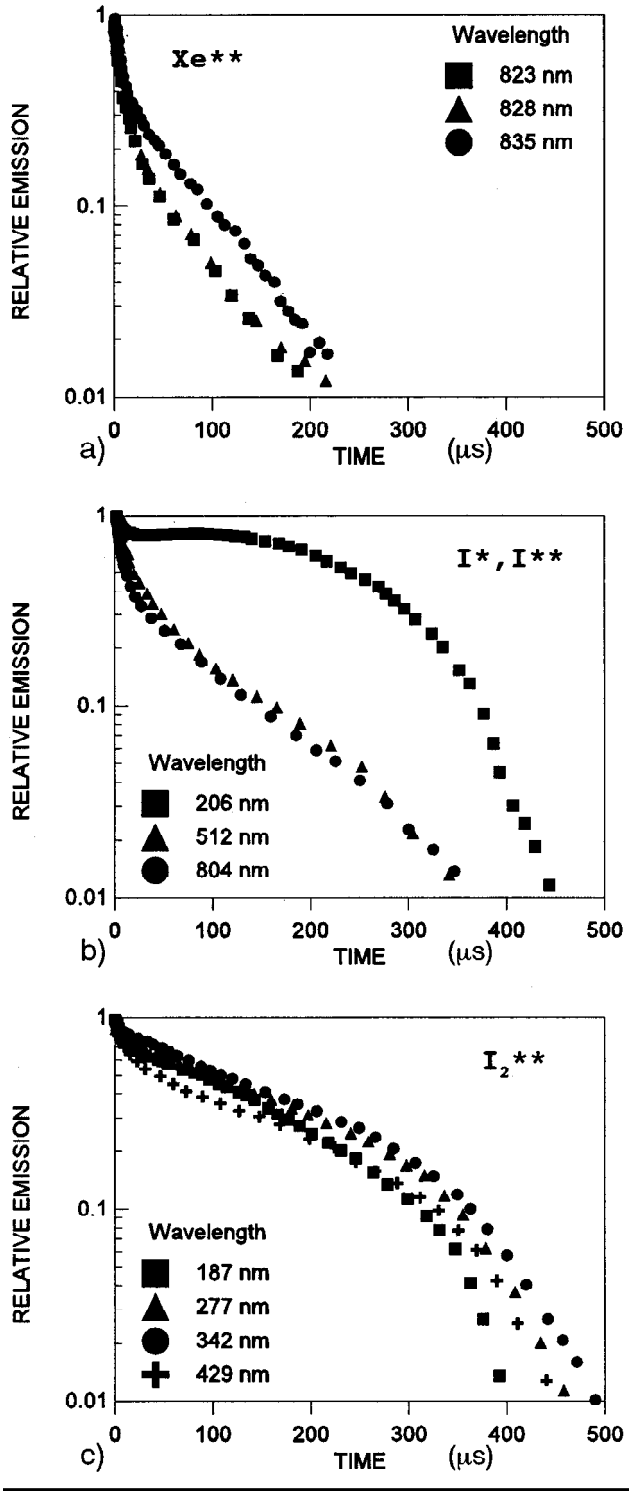

FIG. 6. Emission from a 40 W inductively coupled 0.5 Torr Xe/≈0.3 Torr I_2 time modulated discharge: (a) Xe**, (b) I*, and I**, (c) I_2^{**}.

plied microwave pulses to the afterglow with the intent to heat the electrons, reduce the rate of electron-ion recombination, and so reduce the emission from states populated by recombination. We observed a negligible change in emission at 804 and 206 nm in atomic iodine following electron heating in the afterglow. The implication is that electron ion recombination is not an appreciable source of excitation of $I(^2P_{3/2})$ or higher states in the afterglow.

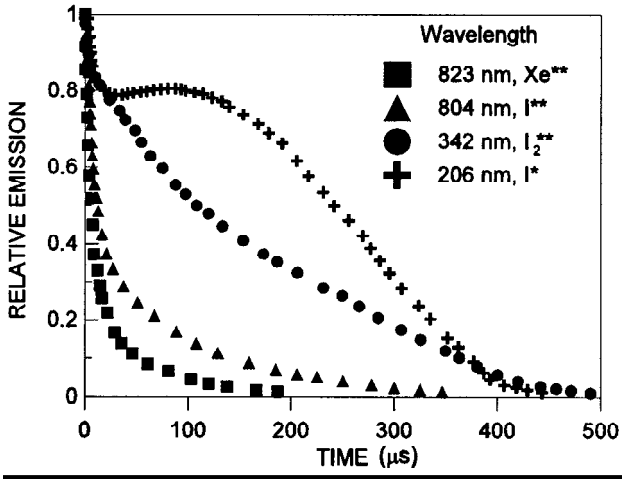

FIG. 7. Emission of Xe** (823 nm), I** (804 nm), I_2^{**} (342 nm), and I* (206 nm) at 40 W for an inductively coupled 0.5 Torr Xe/≈0.3 Torr I_2 time modulated discharge.

If $I(^2P_{3/2})$ is dominantly formed by excitation transfer from Xe metastables, then the I* emission should rapidly decrease when the metastables are depleted. Since the opposite is observed, $I(^2P_{3/2})$ increases while excited states of Xe decay to zero, excitation transfer is not a likely source for the iodine states. A similar argument can be made for dissociative excitation transfer from Xe* to I_2, producing I*.

The last process listed which could produce excited states or I in the afterglow is ion-ion neutralization (process 1c). In order for this process to be the source of $I(^2P_{3/2})$, there must be an increase in the densities of either I^+, I^-, or both during the afterglow to account for the increase in emission at 206 nm since it is unlikely that the rate coefficient for this process appreciably changes on the time scales of interest. I^- is dominantly formed through dissociative attachment to I_2

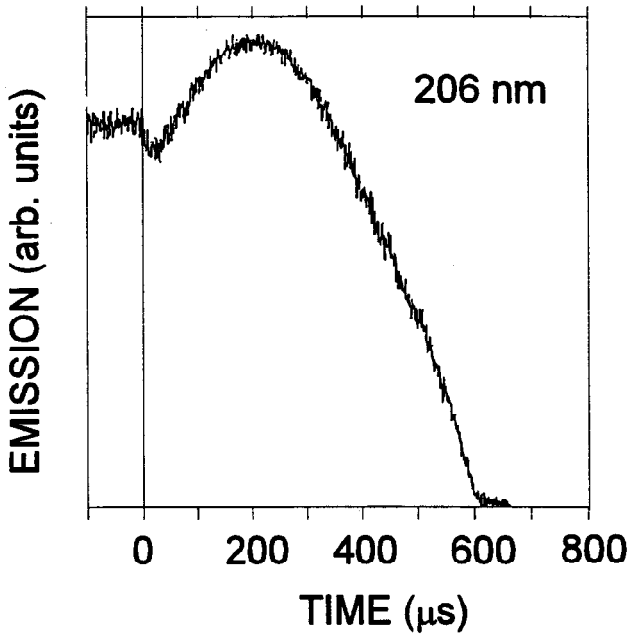

FIG. 8. $I^*(^2P_{3/2} \rightarrow {}^2P^0{}_{1/2})$ emission (206 nm) for a 50 W (0.5 Torr Xe/≈0.3 Torr I_2) time modulated discharge. Scaling is linear.

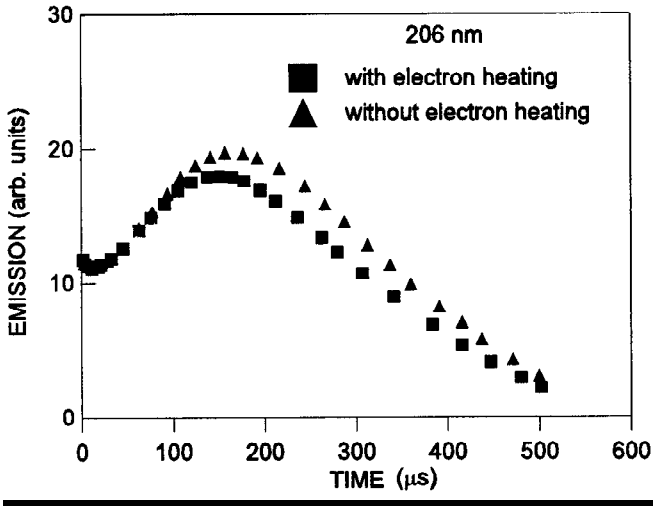

FIG. 9. I* (206 nm) emission with normal time modulation and with an electron heating component in the afterglow. Data taken at 55 W (0.5 Torr Xe/≈0.3 Torr I_2).

$$e + I_2 \rightarrow I^- + I. \tag{2}$$

Since the rate coefficient for this process increases with decreasing electron temperature, the thermalization of electrons during the afterglow could result in an increase in I^- production. The I^+ density could also increase in the afterglow through the charge exchange reaction of

$$Xe^+ + I \rightarrow Xe + I^+. \tag{3}$$

The difference between the ionization potentials of xenon and atomic iodine is 1.68 eV, while I^+has an excited state at 1.70 eV. It is not clear, though, that this process would increase during the afterglow compared to prior modulation of the discharge.

The hypothesis that the 206 nm emission increases due to an increase in I^- followed by ion-ion neutralization with

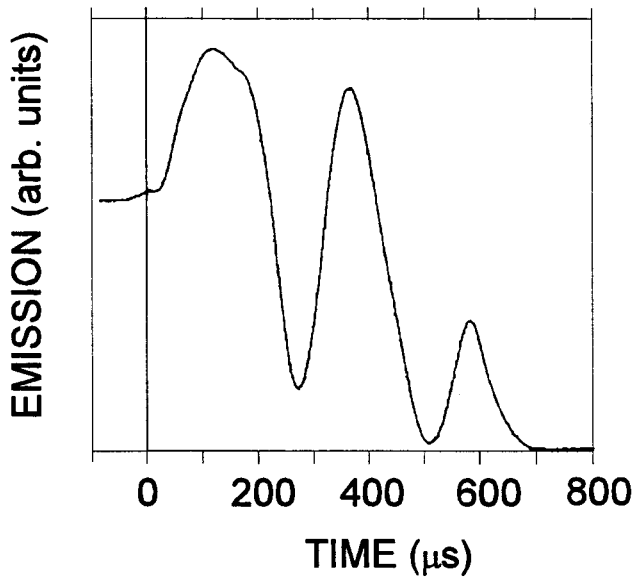

FIG. 10. Interferometry of electron density at 55 W (0.5 Torr Xe/≈0.3 Torr I_2). Scaling is linear.

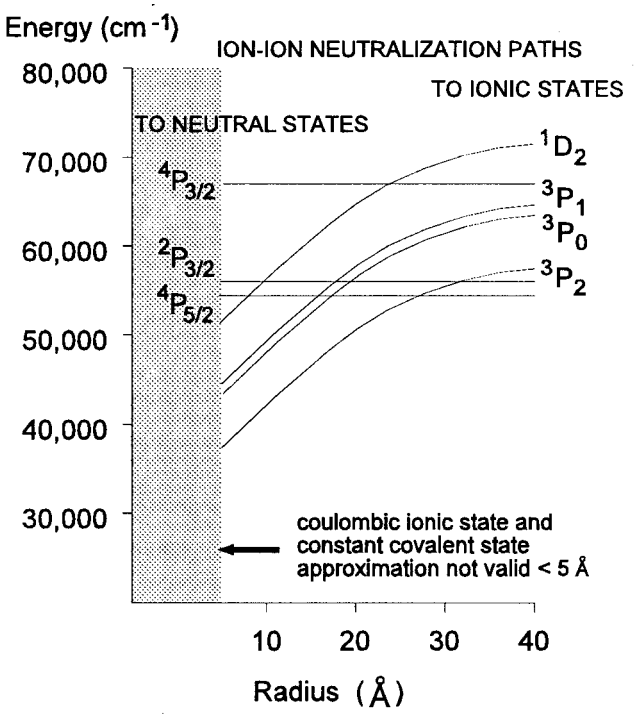

FIG. 11. Schematic potential energy diagram for selected states of I_2.

I^+ depends on electron cooling in the afterglow. Preventing the complete thermalization of electrons in the afterglow should therefore reduce the 206 nm emission peak. Since we received a null result using pulsed microwave heating, we used the alternative method of electron heating during the afterglow by not fully modulating the power off. If the dissociative attachment rate of I_2 increases due to the thermalization of electrons, then preventing electrons from thermalizing in the afterglow should decrease I^- production and hence also decrease emission at 206 nm. This, in fact, was the observed trend, as shown in Fig. 9. Microwave interferometry of the electron density during the afterglow confirms that the electron density does not fully recombine over the time scale of interest, thereby providing feedstock for continued generation of I^-. See Fig. 10. The changing rate coefficient for process (2) due to the thermalization of electrons contributes to the behavior of the 206 nm emission in the afterglow.

The energetics of the ion-ion neutralizations may also favor population of $I(^2P_{3/2})$. For example, if we apply the Landau–Zener theory for ion-ion neutralization,[14–16] the maximum energy available for excitation of the neutral products is the difference between the ionization potential (10.45 eV) and electron affinity (3.06 eV) of atomic iodine, which is 7.39 eV. For example, schematic potential curves are shown in Fig. 11. The ion-pair consisting of I^- and I^+ ($^3P_2$), which is the ion ground state, can indeed energetically access the $I(^2P_{3/2})$ state with a small exothermicity, whereas the $I(^4P_{3/2})$ state, producing emission at 804 nm, is energetically inaccessible. Therefore, if $I^+ + I^-$ neutralization during the afterglow is a major source for $I(^2P_{3/2})$ and is responsible for an increase in the density of this state, we should see an increase in emission at 206 nm but we should not see a

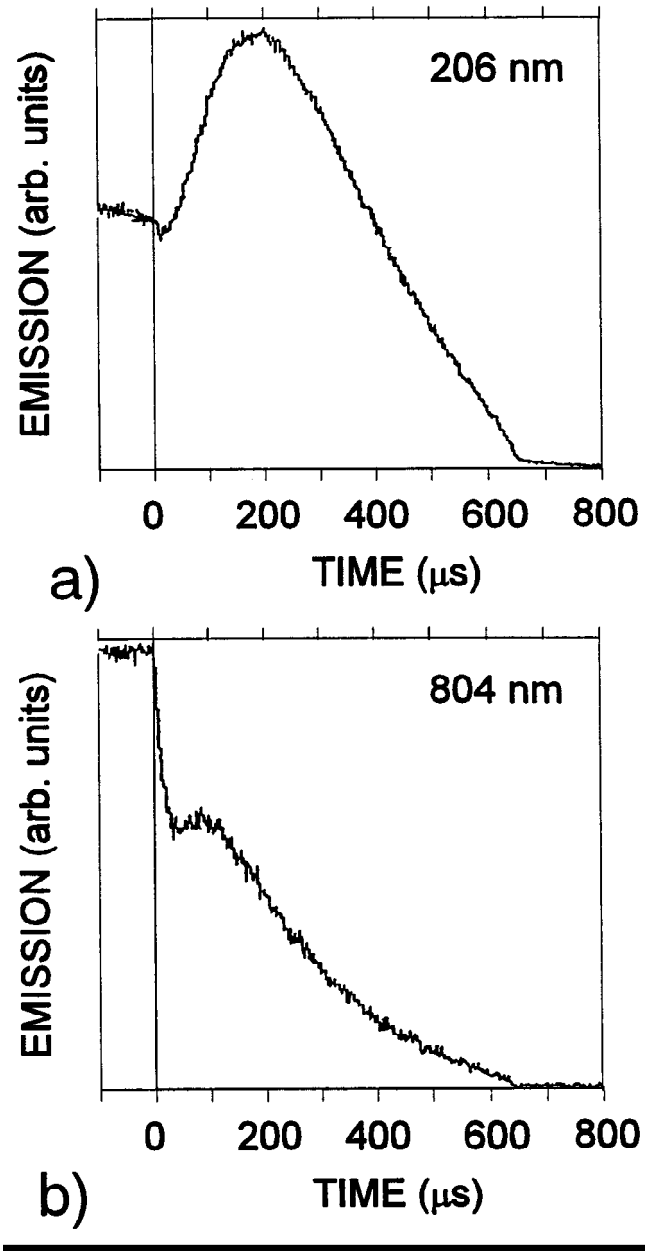

FIG. 12. Emission for a 55 W (0.5 Torr Xe/≈0.3 Torr I_2) time modulated discharge: (a) $I^*(^2P_{3/2}\rightarrow{}^2P_{1/2})$ 206 nm, (b) $I^{**}(^4P^0{}_{3/2}\rightarrow{}^4P_{5/2})$ 804 nm. Scaling is linear.

commensurate increase in the density of $I(^4P_{3/2})$ and emission at 804 nm. This is, in fact, our observation.

Ion-ion neutralization originating from $I^+(^1D_2)$ can energetically access $I(^4P_{3/2})$ and generate emission at 804 nm in the afterglow. Although we cannot selectively control the generation of excited states of I^+, one can expect that a larger fraction of I^+ will be in excited states with higher power deposition. If ion-ion neutralization is a dominant source of excited states of neutral iodine, then increasing power deposition during the on cycle of the modulated discharge should produce more excited states of I^+, and so produce higher excited states of I during the afterglow. We tested this hypothesis by increasing power deposition and monitoring emission from $I(^4P_{3/2})$ at 804 nm. The results, shown in Fig. 12, do indeed show a small maximum during the afterglow, presumably due to ion-ion neutralization of $I^+(^1D_2)$. We note that emission from $I(7p,^4P_{3/2})$ at 512 nm, which originates from ion-pair states higher than $I^+(^1D_2)$, did not show any such increase during the afterglow. The ''kink'' in the emission at ≈630 μs in Fig. 12(b) is an artifact of the data acquisition method.

IV. CONCLUDING REMARKS

The optical emissions from excited states of Xe, I_2, and I were observed during the afterglow of pulse modulated rf discharges in Xe/I_2 mixtures. Emission from states of atomic iodine, and $I(^2P_{3/2})$in particular, are observed for hundreds of μs after the power deposition is turned off and the electrons cool. Under a wide range of operating conditions, emission from this state at 206 nm has a maximum during the afterglow. By comparing the time dependent emissions from I_2^*, Xe*, and other states of I*, we can eliminate excitation transfer, electron impact and electron-ion recombination as major sources which contribute to the increase in $I(^2P_{3/2})$ during the afterglow. Our experimental observations are, however, consistent with ion-ion neutralization between I^- and $I^+(^3P_2)$ as being the source of $I(^2P_{3/2})$. The increase in the density of I^-, the precursor state, during the afterglow is attributed to an increase in dissociative attachment of I_2, a rate which increases as electrons thermalize during the afterglow.

ACKNOWLEDGMENTS

The authors thank Professor J. T. Verdeyen for his advice during the experimental program. Appreciation is given to the Palace Knight Program of the US Air Force for their support of P.N.B. Experimental supplies and funding were provided by Wright Laboratory at Wright–Patterson AFB and the National Science Foundation (ECD 89-43166). Support for M. Kushner was provided by the National Science Foundation (ECS 94-04133).

[1] *Excimer Lasers*, edited by Ch. K. Rhodes (Springer, Berlin, 1979 & 1984).
[2] P. N. Barnes and M. J. Kushner, J. Appl. Phys. **80**, 5593 (1996).
[3] H. Hemmati and G. J. Collins, J. Appl. Phys. **51**, 2961 (1980).
[4] J. J. Ewing and C. A. Brau, Appl. Phys. Lett. **27**, 557 (1975).
[5] S. P. Mezyk, R. Copper, and J. Sherwell, J. Phys. Chem. **97**, 9413 (1993).
[6] R. Cooper, F. Grieser, and M. C. Sauer, Jr., J. Phys. Chem. **81**, 1889 (1977).
[7] K. Tamagake, D. W. Setser, and J. H. Kolts, J. Chem. Phys. **74**, 4286 (1981).
[8] N. K. Bibonov, I. P. Vinogradov, and L. D. Mikheev, Sov. J. Quantum Electron. **13**, 516 (1983).
[9] B. V. O'Grady and R. J. Donovan, Chem. Phys. Lett. **122**, 503 (1985).
[10] H. Hemmati and G. J. Collins, Chem. Phys. Lett. **67**, 5 (1979).
[11] M. C. Sauer, W. A. Mulac, R. Cooper, and F. Grieser, J. Chem. Phys. **64**, 4587 (1976).
[12] M. Martin, C. Fotakis, R. J. Donovan, and M. J. Shaw, Nuovo Cimento **63B**, 300 (1981) as cited in Ref. 16.
[13] H. Massey, *Negative Ions* (Cambridge University Press, Cambridge, 1976).
[14] R. E. Olson, J. R. Peterson, and J. Moseley, J. Chem. Phys. **53**, 3391 (1970).
[15] R. E. Olson, F. T. Smith, and E. Bauer, Appl. Opt. **10**, 1848 (1971).
[16] M. J. Kushner, J. Appl. Phys. **54**, 39 (1983).